encapsulated. The report of the charring depths is taken into account for further comparison. The experiments under consideration are compartment experiment campaigns with CLT panels. The use of CLT products, which exhibit bond line integrity throughout the fire duration, would allow for an improved comparison but due to currently available product limitations, such data are not available yet. In addition to experimental data, comparison to predictions presented by Wade and Wade *et al.* [5, 35] were made.

Subsequently, two experimental campaigns were identified appropriate for the validation of the TiCHS-model. The series have been performed and documented by McGregor [18], Medina [19] and Su *et al.* [20]. From the documented compartment experiments, a further selection was done to cover the range of combustible surfaces in the compartments. The description of the share of the combustible surface refers to the floor area as done typically for the movable fuel load. Table 2 summarizes details of the compartment experimental campaigns where baseline experiments have been performed with non-combustible (NC) enclosure surfaces prior to experiments leaving between 30% and 340% of the structural timber unprotected. It should be noted that in the experiments, various temperature measurements were taken. In the following, the reported mean gas temperature measurements were considered as benchmark. Further, it should be noted that the measurements of the HRR typically experience a time delay, which was considered by shifting the 1 MW point manually to the flashover time observed by the temperature measurements.

4.2 Baseline experiments

The experiments I and II were considered as baseline experiments which were similar to experiments III to VI but without any structural timber. The experiments with exposed structural timber showed increasing shares of the unprotected surfaces between 30% (experiment III) and 340% (experiment VI) referring to the floor area, see Table 2. The movable fire load of the corresponding experiments was similar, thus, it can be expected that the differences in the experiments can be attributed to the structural fire load.

In a first run, a zone-model was set up with appropriate enclosure materials, i.e. gypsum linings and softwood material. Subsequently, the temperature prediction for the HRR measured in the compartment experiment was done and reached a reasonable agreement when the heat of combustion was set to 12.1 MJ/kg, as suggested by Wade *et al.* [35]. No further reduction by *e.g.* a combustion efficiency was done. Thus, the combustion efficiency for the particular experiments can be estimated to:

$$\chi = \frac{\Delta H_{zm}}{\Delta H_{dw}} = \frac{12.1}{17.5} = 0.7 \tag{11}$$

where:

χ is the combustion efficiency factor;

ΔH_{zm} is the heat of combustion used in the zone model, in MJ/kg;

ΔH_{dw} is the heat of combustion (upper heating value; dry wood) of the fuel load, in MJ/kg.

The heat of combustion of timber is taken from Eurocode [1], which refers normally to dry material. Thus, the combustion takes into account the reduced heat of combustion by non-dry material and the creation of soot by the combustion efficiency factor. In Figure 12 and Figure 13,

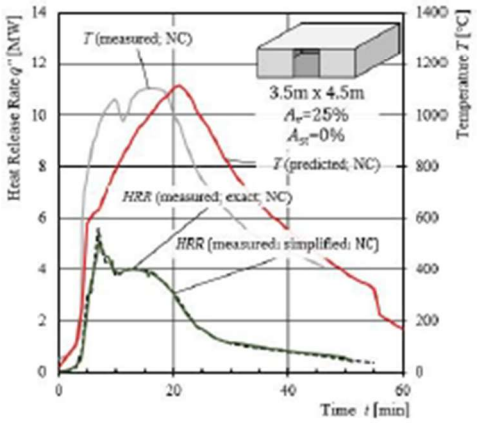

Figure 12: Predicted and measured temperatures for the HRR in baseline experiment I (NC).

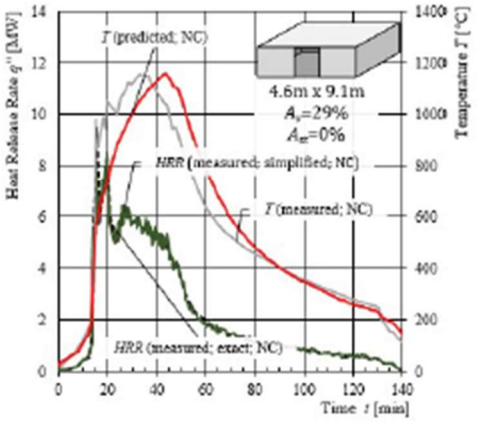

Figure 13: Predicted and measured temperatures for the HRR in baseline experiment II (NC).

the baseline experiments with the input to the zone-model (HRR simplified) and the predicted temperature for this non-combustible (NC) enclosures is provided in comparison to the measured compartment temperature. For both cases, the predicted temperature increase is slightly underestimated which is believed to cause the delay of the peak temperature. Overall, a good agreement of the prediction can be stated.

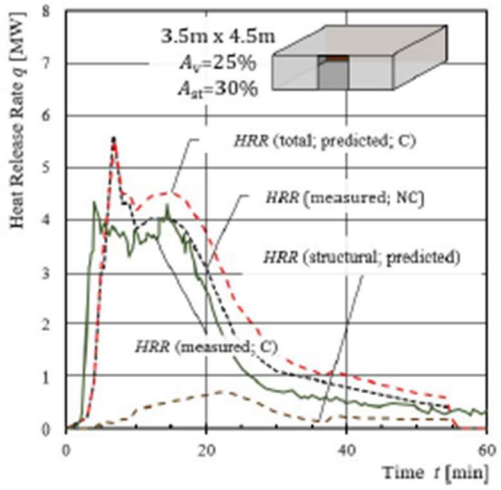

Figure 14: Predicted and measured HRR for experiment III.

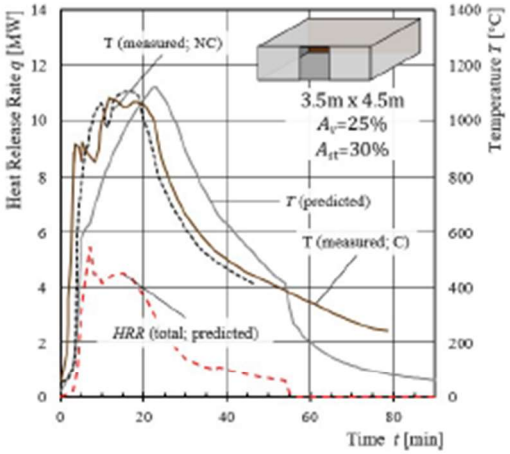

Figure 15: Predicted and measured temperatures for the predicted total HRR for experiment III.

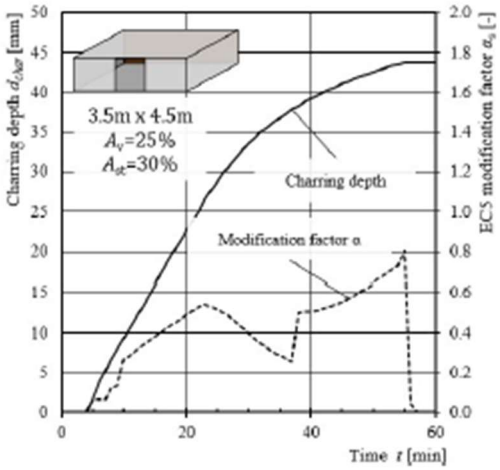

Figure 16: Predicted charring depth and modification factor α for considering the charring behaviour as function of time for the experiment III.

4.3 Exposed structural timber surface 30%

The experiment III had its rear wall exposed, which represents 30% of the floor area. Figure 14 shows the predicted HRR by the TiCHS-model in comparison to the HRR by the baseline experiment II and the measured HRR. Interestingly, it appears that the baseline experiment (NC) showed a HRR excessive the case with the exposed rear wall (C), the green curve in Figure 14. However, the agreement of the predicted HRR is still well and predicts the start of the decay very well. The temperature predictions by the zone-model are provided in Figure 15 and are in good agreement with the peak temperature slightly delayed as for the baseline experiment II (NC), see Figure 13. The development of the charring depth is shown in Figure 16 with a final value of about 44 mm. In the experiment III, the reported charring depth was between 21 mm and 44 mm.

4.4 Exposed structural timber surface 100%

The experiment III had its ceiling exposed, which represents 100% of the floor area. In the experiment, partial fall-off of the CLT's outer lamella was observed after about 40 min, which caused an increase of the HRR, see Figure 17. Until this point, the predicted HRR shows a good agreement. As observed already for the baseline experiment I, the peak temperatures are predicted with a delay, see Figure 18. In Figure 19, the development of the charring depth is given. The charring depth was simulated to reach about 78 mm while measurements indicated values

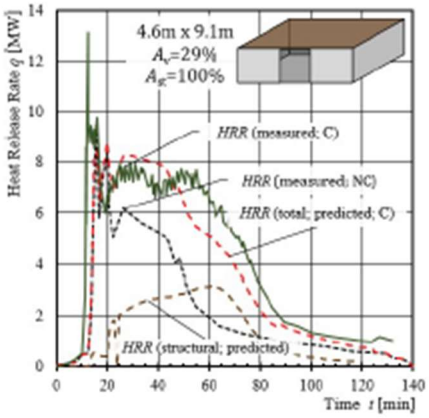

Figure 17: Predicted and measured HRR for experiment IV.

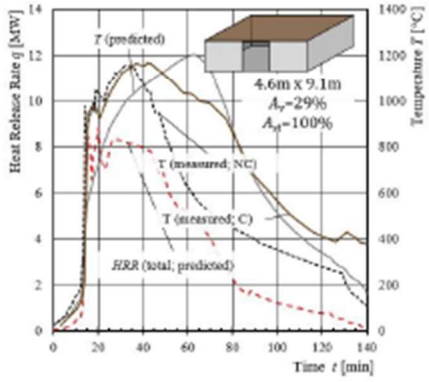

Figure 18: Predicted and measured temperatures for the predicted total HRR for experiment IV.

between about 65 mm and 90 mm. The modification factor for the structural fuel load increases after about 85 min when the char layer starts to get consumed due to the increased oxygen content in the compartment. Apparently, the temperature drop is superior the contribution by this process and the compartment would reach burnout under the condition that the CLT product shows intact bond lines which is not described by the TiCHS-model in its current version.

4.5 Exposed structural timber surface 145%

The experiment V had two opposite walls exposed, which represents 145% of the floor area. In the experiment, fall-off of the CLT's outer lamella was observed after about 40 min, which caused an increase of the compartment temperature, see Figure 21. The recording of the HRR failed after about

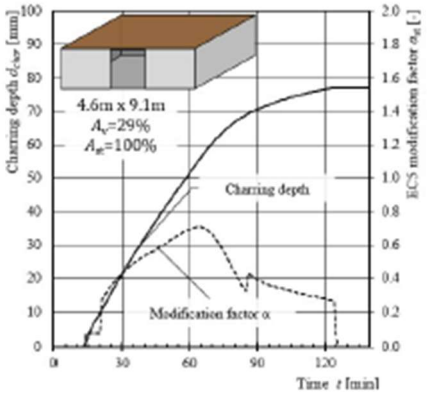

Figure 19: Predicted charring depth and modification factor α for considering the charring behaviour as function of time for the experiment IV.

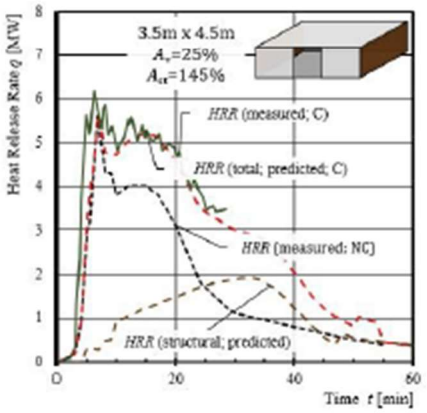

Figure 20: Predicted and measured HRR for experiment V.

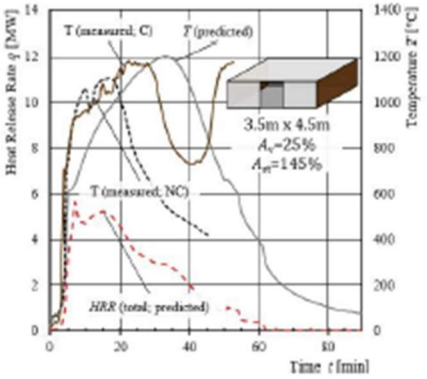

Figure 21: Predicted and measured temperatures for the predicted total HRR for experiment V.

30 min but, until this point, it shows a good agreement with the predictions by the TiCHS-model. The begin of the decay could be predicted fairly well considering the delay of the HRR and the peak HRR and peak temperature, see Figure 20 and Figure 21, respectively. In Figure 22, the development of the charring depth is given. The modification factor for the structural fuel load increases after about 45 min when the char layer starts to get consumed due to the increased oxygen content in the compartment. Apparently, the temperature drop is superior the contribution by this process and the compartment would reach burnout if no fall-off of CLT layers would occur.

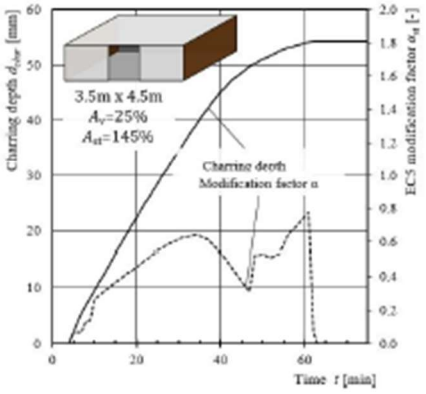

Figure 22: Predicted charring depth and modification factor α for considering the charring behaviour as function of time for the experiment V.

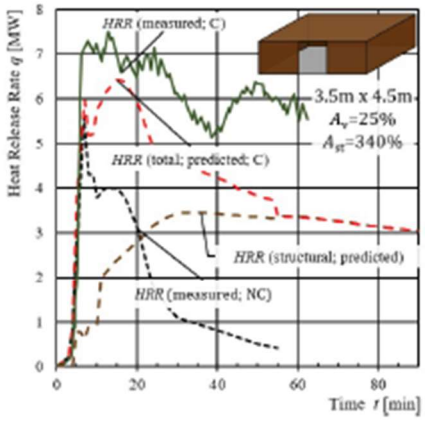

Figure 23: Predicted and measured HRR for experiment VI.

4.6 Exposed structural timber surface 340%

The experiment VI had its ceiling and all walls exposed, which represents 340% of the floor area. This means, all structural timber was left unprotected. In the experiment, fall-off of the CLT's outer lamella was observed after about 40 min, which caused an increase of the HRR, see Figure 23. The predicted HRR underestimates the measured HRR to a limited extent. The decay could be predicted fairly well until the fall-off of charring lamellas caused re-growth of the fire, which was terminated manually after about 60 min. The corresponding temperature measurements are given in Figure 24, which agree well with the measured results. In Figure 25, the development of the charring depth is given. Apparently, no decay of the charring can be expected. The prediction of no burnout is in agreement with corresponding simulations by Wade [5]. The modification factor for

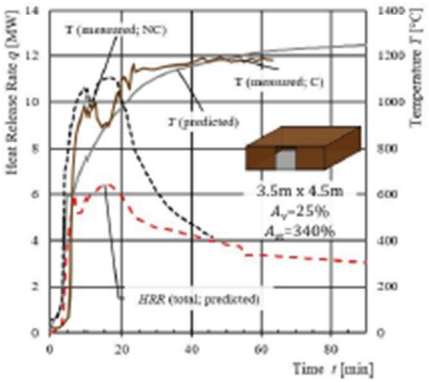

Figure 24: Predicted and measured temperatures for the predicted total HRR for experiment VI.

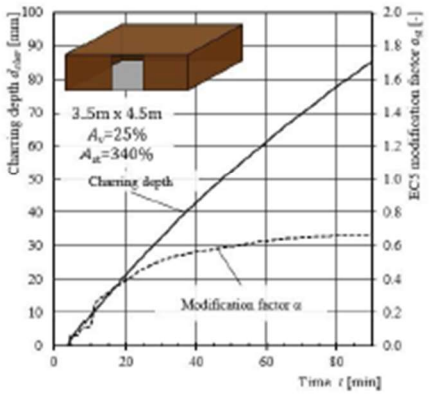

Figure 25: Predicted charring depth and modification factor α for considering the charring behaviour as function of time for the experiment VI.

the structural fuel load does not exceed $\alpha_{st} = 0.7$ during the 90 min. However, it should be observed that no phase with oxygen concentration exceeding 15% was observed during this time. Then, the consumption of the char layer thickness (element 7 in the TiCHS-model) would begin to increase α_{st}.

5 Discussion

A simplified engineering model for the consideration of structural timber in compartment fires was presented in this study. It considers the conversion of the source material, i.e. the structural timber, to a thermally modified layer, commonly known as char layer. The release of combustible volatiles occurs only to a small amount directly from the structural timber but mainly by the decomposition of the char layer. The modification of the structural timber implies the creation of a new material with a significantly less density, about 55% of the dry source material, but a significantly higher heat content, about 170% of the dry source material. From a study on the char layer material by bomb calorimetry [6] it became evident that, the heat content can be assumed to be constant but the density of the char layer density varies between experiments and over its depth. The density of the char layer is reported in literature with a large range, about 50% by Hankalin *et al.* [36] and between 30% and 20% for pine by Tran *et al.* [37]. The application of advanced methods in Eurocode [7] suggests a variable density over the char layer depth with a mean density of about 23% after two hours of standard fire exposure [6]. Considering the large range of data between 50% and 20% and the importance of the char layer acting to the energy storage, the char layer was deeper analysed in this study. A dependency on the decay, i.e. the loss of density, of the char layer was observed. A relationship was determined between the decay and the char layer depth implicitly related to the fire exposure and duration. The dependency was developed by data from char layer characteristics from experiments in fire resistance test furnaces, under a radiant heat panel and a compartment experiment. Together with data available in the literature documenting the pyrolysis and the well-documented production of char coal, a framework was developed to describe the behaviour of structural timber in fire. The mass loss and the specific heat content related to the density can be utilized to describe the potential energy release. Consequently, the developed Timber Charring and Heat Storage model (TiCHS-model) can describe the contribution to the fire dynamics by the structural timber and the char layer, respectively. The TiCHS-model comprises seven elements. The most important contribution to the compartment fire by combustible volatiles originates by the char layer during its decay. It appears important that smouldering and glowing combustion, in contrast to flaming combustion, is insignificantly dependent on the availability of oxygen. The limited dependency of the char combustion by the oxygen concertation can be observed by a slightly reduced fit of the additional data obtained in compartment experiments in comparison to heat panel experiments. The TiCHS-model is able to assess the contribution of structural timber to the fire dynamics by the determination of the structural HRR. Consequently, an iterative approach is followed based on the prediction of the compartment environment, i.e. the temperature and the gas characteristics in the compartment. Calculations were presented comparing the total HRR and the compartment temperature of the proposed procedure and experiments available in the literature. The results in terms of charring depth are about ± 5 millimetre compared to the experimental results. The predictions achieve an overall good agreement unless fall-off of charring layers induce a re-growth of the fire due to the sudden change of the combustion characteristics. These effects can be attributed to the sudden direct exposure of virgin wood and the significantly changed fire exposure of the fallen char layer. By fall-off, the char material is suddenly exposed to an oxygen richer environment at multiple sides. For the correct description of the combustion of char material on the floor, further information is essentially needed. The radiation from the surface flaming to other combustible members than the origin is currently not explicitly considered. Consequently, the model should not be used for compartments with exposed structural timber walls that are narrower than in the experimental data used for validation. The consideration of the relative arrangement of structural timber walls will be implemented when further data is available. In the calculations presented in this publication, a combustion efficiency of $\chi = 0.7$ is used while for design purposes a deviating factor may be used to allow for a conservative result. This combustion efficiency factor χ does not cover the factor α_{st} to consider the combustion behaviour of structural timber. The latter describes the delayed combustion caused by the char layer creation.

6 Conclusions

After the validation of the TiCHS-model by means of compartment experiments, the following statements can be made:

- The TiCHS-model can be used to predict the HRR together with a zone-model;
- The TiCHS-model is able to predict burn-out and the charring-depth;
- The TiCHS-model did predict the charring depth slightly conservative but in good agreement with the observations in the experiments;
- The TiCHS-model allowed the determination of the factor α_{sf} to describe the combustion behaviour of structural timber.

It should be noted that the TiCHS-model in its current form does not consider a potential failure of the bond line, i.e. fall-off of charring layers. In a future model, it is planned to implement this feature although it is considered of minor interest as the adhesive industry is about to introduce improved adhesives. An important element to be studied prior to the intended implementation is the combustion characteristics of failed layers, which have been thermally modified sticking to the CLT, partly decomposed in the original location and suddenly exposed to multiple sides and oxygen-rich environments at the floor of the compartment after its fall-off.

In general, it was shown that the predictions using the TiCHS-model reach a good agreement with the measurements in the compartment experiments. Further, a good agreement with the prediction of corresponding simulations available in the literature was achieved. Here it should be noted that the TiCHS-model does not require the definition of a fuel access factor or a corresponding parameter study. Currently, the model is validated for the gas velocities, which occur in compartments with openings on one side. In the future, it is expected that the requirements will be set for superimposing the natural gas flow with imposed gas flow by wind. This is believed to be an important task for medium and high-rise buildings with potential cross-flows.

Acknowledgement: The Swiss National Research Fund (SNF) and IGNIS-Fire Design Consulting are acknowledged for the provided financial resources to allow for the corresponding research. The research team of ETH Zürich including numerous master students are acknowledged for their experimental support.

References

[1] EN 1991-1-2: Eurocode 1: Actions on structures - Part 1-2: General actions – Actions on structures exposed to fire. European Committee for Standardization, Brussels. 2002.

[2] Maag T, Fontana M. Brandversuche an Modulhotels in Holzbauweise. ETH Zurich. 2000.

[3] Hakkarainen T. Post-flashover fires in light and heavy timber construction compartments. Journal of fire sciences. 2002 Mar;20(2):133-75.

[4] Brandon D. Engineering methods for structural fire design of wood buildings: Structural integrity during a full natural fire. Brandforsk Report 2018:2. 2018.

[5] Wade CA. A theoretical model of fully developed fire in mass timber enclosures. Doctoral Thesis, University of Canterbury, New Zealand. 2019.

[6] Schmid J, Richter F, Werther N, Frangi A. Combustion characteristics of structural timber compartments in the steady-state fire phase. Fire Technology. Submitted 2020.

[7] EN 1995-1-2: Eurocode 5: Design of Timber Structures – Part 1-2: General – Structural Fire Design. European Committee for Standardization, Brussels. 2004.

[8] Friquin KL. Charring rates of heavy timber structures for Fire Safety Design: A study of the charring rates under various fire exposures and the influencing factors. 2010

[9] Crielaard R. Self-extinguishment of cross-Laminated timber. Master Thesis, University of Delft, Netherlands. 2015.

[10] Schmid J, Santomaso A, Brandon D, Wickström U, Frangi A. Timber under real fire conditions - the influence of oxygen content and gas velocity on the charring behavior. SIF'16, Structures in Fire 2016, Princeton, U.S.A. 2016.

[11] Knaust C, Kusche C. Entwicklung eines Verfahrens zur Bestimmung der Verbrennungseffektivität für Brandlastberechnungen. Fraunhofer IRB-Verlag. 2014.

[12] Schmid J, Fahrni R, Frangi A, Werther N, Brandon D, Just A. Determination of design fires in compartments with combustible structure - modification of existing design equations. Proceedings INTER International Network on Timber Engineering Research, 52, 509-511. 2019.

[13] Putynska CG, Law A, Torero JL. An investigation into the effect of exposed timber on thermal load. In24th Australasian Conference on the Mechanics of Structures and Materials 2016 Nov 30 (pp. 939-944). 2016.

[14] Schmid J, Lange D, Sjöström J, Brandon D, Klippel M, Frangi A. The use of furnace tests to describe real fires of timber structures. In Proceedings of WCTE 2018—world conference on timber engineering. 2018.

[15] Schmid J, Brandon D, Werther N, Klippel M. Thermal exposure of wood in standard fire resistance tests. Fire safety journal, 107, 179-185. 2019.

[16] Wade CA, Baker GB, Frank K, Harrison R, Spearpoint M. B-RISK 2016 User Guide and Technical Manual. BRANZ. 2016.

[17] Lennon, T., M. J. Bullock, and V. Enjily. The fire resistance of medium-rise timber frame buildings. World Conference on Timber Engineering. 2000.

[18] McGregor C. Contribution of cross laminated timber panels to room fires (Master thesis, Carleton University). 2013.

[19] Medina AR. Fire resistance of partially protected cross-laminated timber rooms, Master thesis, Carleton University. 2015.

[20] Su J, Lafrance PS, Hoehler MS, Bundy M F. Fire Safety Challenges of Tall Wood Buildings–Phase 2: Task 3-Cross Laminated Timber Compartment Fire Tests. NIST Report A1-010659.1. 2018.

[21] Lange D, Sjöström J, Schmid J, Brandon D, Hidalgo J. A Comparison of the Conditions in a Fire Resistance Furnace When Testing Combustible and Non-combustible Construction. Fire Technol-

ogy. 2020.
[22] EN 1363-1: Fire resistance tests – Part 1: General requirements. European Committee for Standardization, Brussels. 2012.
[23] ISO 834-1: Fire-Resistance Tests – Elements of Building Construction – Part 1: General Requirements. International Organization for Standardization. Geneva, Switzerland. 1999.
[24] Klippel M., Schmid J., Fahrni R., Frangi A. Assessing the adhesive performance in CLT exposed to fire. World conference on Timber Engineering, Seoul. WCTE 2018. South-Korea. 2018.
[25] ISO 5660-1: Reaction-to-fire tests-heat release, smoke production and mass loss rate– Part 1: heat release rate (cone calorimeter method) and smoke production rate (dynamic measurement). International Organization for Standardization. Geneva, Switzerland. 2015.
[26] ASTM E 2058-13, Standard Test Methods for Measurement of Synthetic Polymer Material Flammability Using a Fire Propagation Apparatus (FPA). ASTM International, West Conshohocken. 2013.
[27] Werther, N. Einflussgrössen auf das Abbrandverhalten von Holzbauteilen und deren Berücksichtigung in empirischen und numerischen Beurteilungsverfahren. Doctoral Thesis, Technical University of Munich, Germany. 2016.
[28] EN 1995-1-2: 2nd Draft for revision of Eurocode 5: Design of Timber Structures – Part 1-2: General – Structural Fire Design. European Committee for Standardization, Brussels. 2020.
[29] Bunbury, H. M. (1925). Die bei der trockenen Destillation des Holzes erhaltenen Handelsprodukte, Springer.
[30] Sibulkin M. Heat of gasification for pyrolysis of charring materials. In Fire Safety Science: Proceedings of the First International Symposium (pp. 391-400). (1985).
[31] Mikkola E. Charring of wood. Tutkimuksia-Valtion Teknillinen Tutkimuskeskus (1990).
[32] Spearpoint M, Quintiere J. Predicting the burning of wood using an integral model. Combustion and Flame. 2000.
[33] Chatani Y, Harada K. Measurement of Char Oxidation of a Glue Laminated Timber Material heated by Cone Calorimeter. 2015.
[34] Jervis C. Application of fire calorimetry to understand factors affecting flammability of cellulosic material: Pine needles, tree leaves and chipboard; The University of Edinburgh. 2012.
[35] Wade C, Spearpoint M, Fleischmann C, Baker G, Abu A. Predicting the fire dynamics of exposed timber surfaces in compartments using a two-zone model. Fire technology. 54(4), 893-920. 2018.
[36] Hankalin VI, Ahonen TU, Raiko RI. On thermal properties of a pyrolysing wood particle. Finnish-Swedish Flame Days. 2009 Jan 28;16.
[37] Tran HC, White RH. Burning rate of solid wood measured in a heat release rate calorimeter. Fire and materials. 1992 Oct;16(4):197-206.

17.2 Load bearing capacity of timber members in the fire situation

17.2.1 General

Several **simplified methods** were recently presented by various authors, all referring back to standard fire resistance tests of timber components and the well-established charring rates in the fire resistance tests. A method for the assessment of the time equivalency has been presented recently (Barber et al. 2021). The process is linked to the one-dimensional basic design charring rate of 0.65 mm/min. Thus, the time equivalency can be assessed as:

$$t_{eq} = \frac{d_{\text{char}}}{\beta_0} \qquad \text{Eq. 5}$$

where

t_{eq} is the time equivalent, in min;

d_{char} is the charring depth for the non-standard fire, in mm;

β_0 is the one-dimensional basic design charring rate, in mm/min.

The aforementioned method neglects the reduction of the load-bearing capacity in the fire situation which may be superior to the standard fire if the thermal impact depth is increased in the decay phase.
An **advanced approach** is the prediction of the charring depth considering the fire dynamics and the estimation of the thermal impact on the, see 17.2.2.

17.2.2 Simulation of heat transfer into the structural timber

The thermal material properties of wood provided in standard documents, e.g. EN 1995-1-2 [CEN 2004] are not generally valid properties. As they have been developed (backwards calibrated) for standard fires, their validity may be limited when the design fire, and thus, the heating of the particular timber component, deviates significantly from the EN/ISO fire exposure.
Consequently, in this document, a more flexible tool was used to determine the temperature profile, sometimes referred to as "heat wave", within the timber section. The approach presented in this document uses generally valid Arrhenius functions to model the decomposition of wood and, therefore, the charring depth. Arrhenius equations are widely used by a lot of models to simulate the pyrolysis of timber with different proposals for reactions, sub-reactions and parameters, for example (Fredlund, 1993), (Lautenberger & Fernandez-Pello, 2008), (Mindeguia, 2017) and (Vermesi, et al., 2017). In Mindeguia (Mindeguia, 2017), there are formulas given for the timber thermal properties density ρ, specific heat capacity c and conductivity λ for the Arrhenius method. They are compiled by the ratio of reaction of lignin χl and water χw and the properties of timber, water and char. The production rate of the char layer material (rate γ) is derived by means of a significant density drop when timber is converted. The relative density of

char is assumed 0.2, other references state values from 0.15 (Nussbaumer, 2000) to 0.33 (Spearpoint & Quintiere, 2000).

$$\rho = \rho_s \cdot [1 + \chi_l \cdot (\gamma - 1) + w \cdot (1 - \chi_l)](1 - \chi_l) \cdot \lambda_w \quad \text{Eq. 6}$$

$$c = \frac{(1 - \chi_l) \cdot c_s + \gamma \cdot \chi_l \cdot c_{char} + w \cdot (1 - \chi_w) \cdot c_w}{[1 + \chi_l \cdot (\gamma - 1) + w \cdot (1 - \chi_w)]} \quad \text{Eq. 7}$$

$$\lambda = (1 - \chi_l) \cdot \lambda_s + \frac{\rho_s}{\rho_{char}} \cdot \gamma \cdot \chi_l \cdot \lambda_{char} + \frac{\rho_s}{\rho_w} \cdot w \cdot (1 - \chi_w) \cdot \lambda_w \quad \text{Eq. 8}$$

where

c	is the specific heat capacity;
$char$	is the index for the char layer;
l	is the index for the lignin;
s	is the index for the solid wood;
w	is the index for the wet wood;
λ	is the thermal conductivity, in W/(mK).
ρ	is the density, in kg/m^3.
χ	is the ratio of reaction; in s^{-1}.

For the calculation of the charring rate, an element is considered charred when the additional reaction ratio per time of β-cellulose is maximal. This assumption gives the best results according to Mindeguia (Mindeguia, 2017). Typically, an element gets charred almost instantly when the reaction of β-cellulose started. For this reason, a secondary criterion, that the reaction ratio has to be at least 10%, was introduced. The explicit model of heat transfer (inner node) is schematically shown in Figure 40.

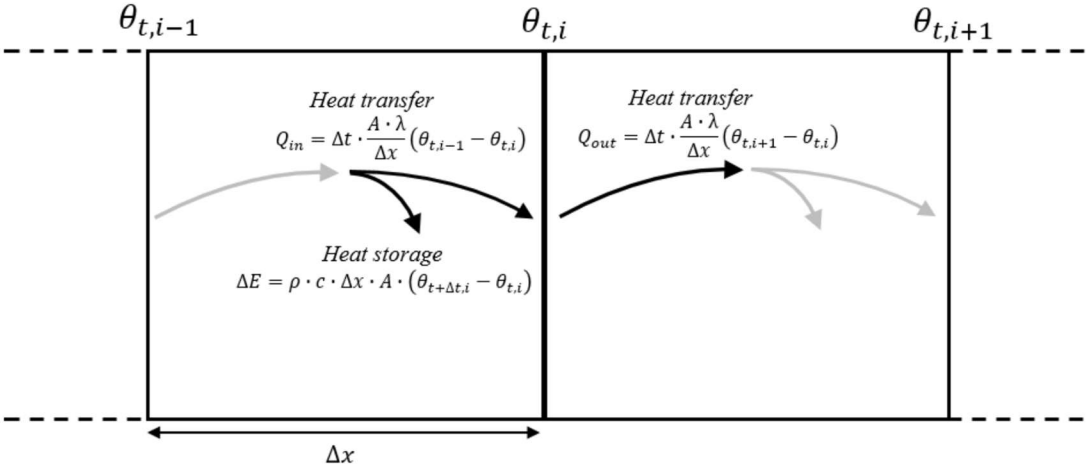

Figure 40: Explicit heat equilibrium in inner node of the material.

The model parameters have been developed and published by Mindeguia [2017] and are shown in Table 15.

Table 15: Arrhenius equation parameters from Mindeguia, 2017.

	Pre-exponential factor A [1/s]	Activation Energy E [kJ/mol]	Reaction Enthalpy H [kJ/kg]
Lignin	5.09E5	164	79
Water	1E20	162	*
Cellulose	4.71E31	333	0
α-cellulose	1.3E10	151	418
β-cellulose	3.2E14	196	418
Hemicellulose	5.78E13	104	0
* -2265 for discrete method, -7000 for analytical method			

17.2.3 Validation of the Heat Transfer Model

The particular code used is a Python code which simulates the heat transfer to the solid and within the solid, i.e. the structural timber. The code was developed based on available material properties and basics of heat transfer. The functionality was validated using standard fire and deviating fire developments including the cooling phase.

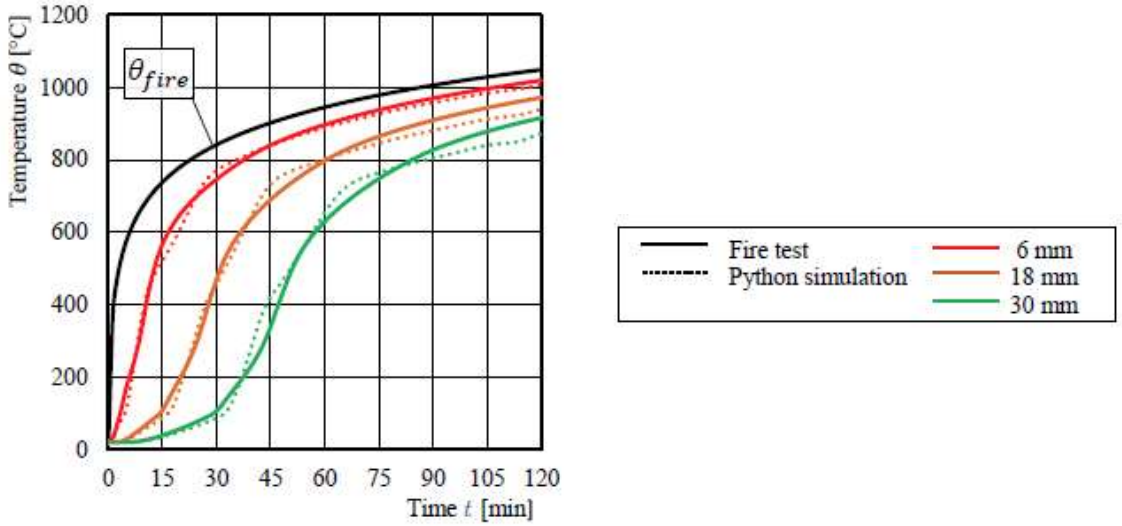

Figure 41: Temperature-time for standard fire (discrete method).

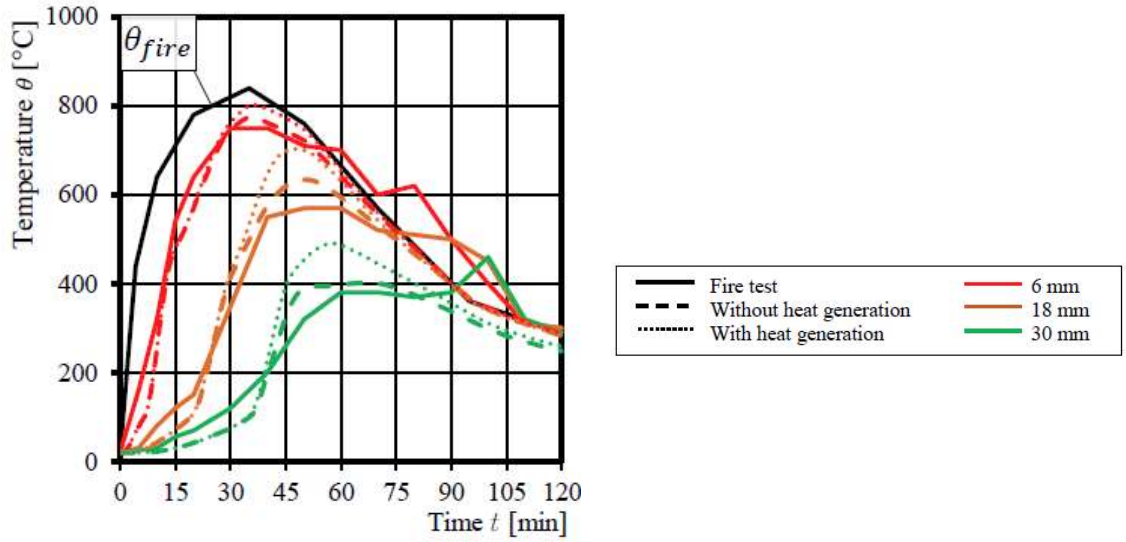

Figure 42: Temperature-time for a design fire (discrete method).

The differences due to the implementation of heat generation and char recession can also be seen in the char rates (Figure 43). Without these effects, the char rate at the beginning is about 0.7 mm/min in both methods, and decreases as the fire temperature declines. The heat generation starts to show an effect after a simulation time of about 20 min, increasing the rate as additional energy is induced. With the given parameters, the chosen criterion of 80% char reaction ratio for char layer regression was not triggered in the simulation with the discrete method. For the analytical method, the char recession takes place very fast in a short time, leading to a jump up of the char rate.

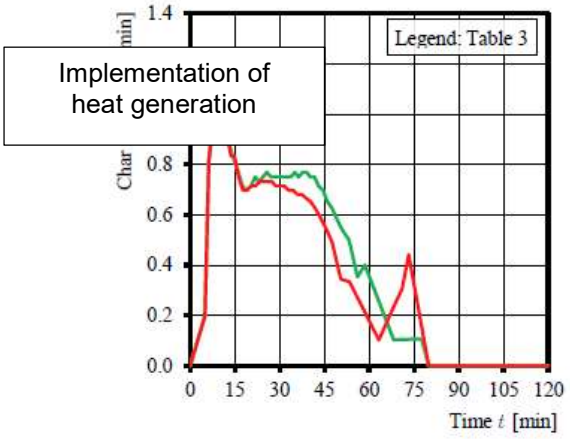

Figure 43: Charring rate vs. time for a design fire (discrete method); without heat generation (red curve) and with heat generation (green curve)

17.3 External flaming

17.3.1 General

The external flaming analysis comprises the analysis of **(a) flame heights and (b) the radiation to neighbouring buildings** (alternatively the legal boundaries). The flame heights are used as an input for the radiation calculation as well as to estimate the risk of exterior fire spread.
The presence of flames outside of a burning compartment is caused by unburned pyrolysis gases leaving the burning compartment. This happens when the (natural) ventilation does not provide enough oxygen to combust all pyrolysis gases that are produced in the compartment due to high temperatures. In general, the external HRR is the difference from the total HRR and the internal HRR, see also Figure 44:

$$HRR_{ext} = HRR_{total} - HRR_{int} \quad \text{Eq. 9}$$

The internal HRR is basically given by the burning objects (total HRR), but may be limited by the oxygen entering through the openings (CCC: compartment combustion capacity). Only in these so-called ventilation-controlled fires the external HRR will be above zero.

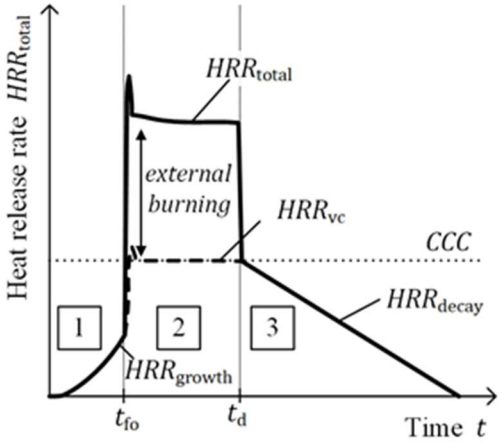

Figure 44: General development of the total heat release (rate) in a fire.

The calculation of flame heights is done based on EN 1991-1-2 [BSI 2002], which is equivalent to Law 1983 and Spearpoint 2008. However, the HRR given in EN 1991-1-2 would not consider the structural HRR. Thus, the HRR used for the flame height calculation is the external HRR given from the auto-extinction analysis.
BR 187 limits the irradiation in the decisive distance to 12.6 kW/m^2, which reflects the ignition limit of wood when exposed to radiation. Babrauskas 2003 proposes 20 kW/m^2 as a limit, reflecting an average for typical building materials.
The calculation bases on the Stefan-Boltzmann-law, which defines the power radiated by a body in terms of its temperature. EN 1991-1-2 provides the necessary formulas and gives guidance on assumptions. The

energy that is received from a radiating surface depends on the distance and orientation. Since every solid with a temperature above 0 K radiates, the actual irradiation is the difference between the radiation received from surrounding surfaces and own radiation losses. For the analysis, it is assumed that the surface at the decisive distance has a temperature of 20° C. The radiation emission from the compartment on fire is modelled according to EN 1991-1-2 and BR 187 by a (virtual) surface at the opening radiating with the compartment temperature. The emissivity for those surfaces is chosen as 1.0. The flames above the window are modelled in a similar way, where EN 1991-1-2 defines a temperature based on the flame length and an emissivity based on the thickness of the flames.

The irradiation limit must be fulfilled at any point on the neighboring building. Assuming that the façade of the neighboring building is parallel to the investigated one (i.e. is at a constant distance), the highest irradiation of a rectangular emitter occurs centrally in front it. However, for multiple sources or when flames are considered, the critical location must be found iteratively. Exemplarily, Figure 45 shows the irradiation at various heights, measured from the top of the radiating opening. Generally, the higher the flames the higher the most critical point. If there are no flames at all, i.e. when the fire is fuel-controlled, the most critical point is at mid-height of the opening.

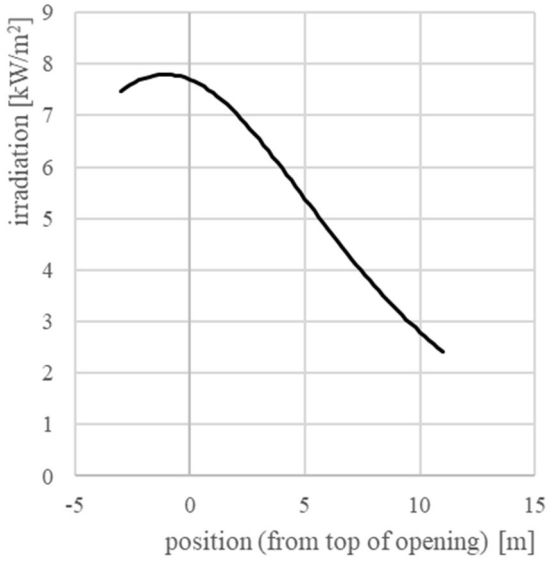

Figure 45: exemplary irradiation over the height, centrally in front of the openings

17.3.2 Consideration of sprinklers

In the current building, water sprinkler will be installed as part of the technical measures of fire safety design. The consideration of sprinklers follows currently available guidance which is given in the present Eurocode and British standards. Typical values of the reliability of installed sprinkler values describe the risk of failure to be not able to effectively suppress a fire effectively.

Following guidance, for the fire design, sprinklers are considered by the modification of the fire load density, while the peak HRR in remains unchanged. This means, that the resulting external HRR and the radiation to a neighbouring building remain changed when a sprinkler is present, despite the reduced risk to observe a fully developed fire.
To consider the effect of sprinklers despite the assumption of a fully developed fire, the Approved Document B (ADB) suggests to divide the required distance to the legal boundary or the decisive distance (e.g. to the neighbouring building façade) in halves. This is equivalent to double the amount of allowed unprotected area (ADB clause 13.21). Thus, the present analysis considers the effect of sprinklers by halving the required boundary distance as proposed in ADB.

18 Annex R – Fire Safety requirements for timber buildings

18.1 Limitations

Classification done in this document provided by IGNIS is not necessarily directly related to classification according to (European) fire resistance testing and classification according to EN 13501-1 and EN 13501-2 or other classification standards unless explicitly stated. The fire design and the resulting requirements for the building components may have impact on the execution, acoustics and architecture. The corresponding information flow of eventually needed changes should be ensured by the project lead. It is important to underline that the assessment given in this document can only be applied for the project considered in this document. If products (brands, types) are mentioned, they represent examples and can be exchanged when a similar performance is provided. If products that are specified in this document are replaced by other products, their performance need to be assessed accordingly.

18.2 Identification of the requirements for the design

The requirements for the connections and joints shall fulfil the building regulations relevant for the given project. As building regulations aim for life safety as major objective, other objectives are not necessarily specified. The definition of safety objectives exceeding the building regulations may have favourable impact on the performance in and after building fires and insurance costs. However, it is expected that those additional safety objectives have impact on the design of the building in general and on detailing.
The definition of additional safety objectives is finally up to the fire safety engineer and the building owner. The fire resistance rating with respect to R, E and I may be equal or different for fire from one or the other side; consequently, the definition is part of the fire engineer's work.
The following requirements can be listed with respect to fire performance of building components:

R-Resistance in fire: The load-bearing resistance is verified for a relevant design load defined by the fire safety engineer and/or the structural engineer, assessed by testing or calculation. As the design fire, typically, the EN/ISO standard fire time-temperature curve is assumed which is considered as comparative measure. It should be noted that the fire resistance classification is done in certain steps (levels), e.g. multiples of 30 min and specified as R30, R60, R90 or R120. Furthermore, it should be considered that the verified fire resistance is valid for a particular loading. The latter means that the same component may be appropriate for a high fire resistance with respect to the time for a low mechanical loading while the contrary is not automatically valid. For structural timber, the remaining (uncharred) section is the most relevant variable for the assessment of the load-bearing capacity in the fire situation. For structural steel, the section temperature is decisive for the load-bearing capacity.

E-Integrity in fire: The integrity of a component or a joint or connection between adjacent components addresses its or their performance in the fire situation with respect to the **penetration** through the detail by **hot gases**. Hot gases may lead to fire spread on the other side of the member. This function has to be verified for compartmentation at the boundaries of compartments.

I-Insulation: The insulation of a component or a joint or connection between adjacent components addresses its or their performance in the fire situation with respect to the **conduction** of temperature through the detail. The temperature rise can be verified by testing (limitation of a temperature increase by 140 K (mean) and 160 K (max), respectively), calculated by simplified models or simulated using advanced models (e.g. FEM).

K-encapsulation: The European system of so-called K-classes for the fire protection performance of coverings is defined in EN 13501-2 based on full-scale furnace testing in horizontal orientation according to EN 14135. Beside the measured temperature criterion behind the protective lining after different time intervals (10, 30 and 60 minutes), no collapse, burning (discoloration) on the wood-based panel substrate or falling parts are allowed. Two types of K classes are defined, depending on the substrate behind the protective material. Class K_1 includes substrates with density less than 300 kg/m^3, while class K_2 includes all substrates, so in practice it is sufficient to verify K_2 classes for protection of wood. Currently, encapsulation can only be achieved by protection by fire boardings. Beside the temperature rise behind the panel, the discoloration near fire protection boarding panels and mechanical fixations (screws) is taken into account for the assessment of the encapsulation function.

B-Burnout: The burnout of a compartment may be required in building regulation or guidance depending on the building class (typically related to the building height) and/or its occupation. Regardless the building material, total burnout cannot be guaranteed but its likely occurrence can be assessed by the application of design models. Consequently, building and detail design may be adjusted based on this criterion. Typically, for timber buildings, this is a criterion explicitly requested for higher or more complex buildings. However, the general application of standard fire resistance ratings (specified in minutes) may still be sufficient to achieve burnout.

GS-Glowing and smouldering combustion: The prevention of glowing and smouldering combustion is a typical element, which supports the achievement of likely burnout. Detailing appears to be crucial to reduce the risks for unrecognised glowing and smouldering combustion after a fire event, as its detection requires special skills and equipment of the fire services. The limitation of this criterion requires the limitation of charring and gas flow (continuous paths through the construction).

CH-Charring: The prevention of charring behind a fire protection system may be required by building regulations or by the model assumptions. Consequently, the temperature limit behind a fire boarding may be adopted to a limit equal or lower than 300° C, recognised in e.g. Eurocode as charring temperature. The protection ability can be determined by means of a fire resistance encapsulation test and a corresponding classification (K-classes) or, if applicable, simplified or advanced modelling.

In the current project, the following max temperature should be set in cooperation with building control:

(1) The temperature on the top side of the CLT floor panels should not exceed 300° C (to prevent contribution of timber to the total fuel load in the case of fire).
(2) The temperature at the CLT support area should not exceed 250° C (to avoid additional deflections at the support due to charring). The critical temperature is verified by means of thermal finite element simulations.

LST-Limiting Steel Temperature: The load-bearing capacity of steel members is correlated to member temperature with a significant drop from about 400° C regardless the heating rate. With respect to the load-bearing capacity of the steel works, a temperature limit for the cross-section must be defined for all design details by the structural engineering team. This limit must be considered for the planning of the configuration of the fire boarding. It should be noted that this temperature limit is eventually above the pyrolysis and charring temperature of timber. Consequently, charring can be expected for corresponding details where the steel elements are in direct contact with timber elements and a steel temperature limit higher than the pyrolysis temperature is used for the design of the detail. This criterion is not a standardised criterion.